



OPEN

The effect of quaternary ammonium polyethylenimine nanoparticles on bacterial adherence, cytotoxicity, and physical and mechanical properties of experimental dental composites

Grzegorz Chladek^{1✉}, Izabela Barszczewska-Rybarek², Marta Chrószcz-Porębska² & Anna Mertas³

A significant problem related to the functioning of resin-based composites for dental fillings is secondary or recurrent caries, which is the reason for the need for repeated treatment. The cross-linked quaternary ammonium polyethylenimine nanoparticles (QA-PEI-NPs) have been shown to be a promising antibacterial agent against different bacteria, including cariogenic ones. However, little is known about the properties of dental dimethacrylate polymer-based composites enriched with QA-PEI-NPs. This research was carried out on experimental composites based on bis-GMA/UDMA/TEGDMA matrix enriched with 0.5, 1, 1.5, 2 and 3 (wt%) QA-PEI-NPs and reinforced with two glass fillers. The cured composites were tested for their adherence of *Streptococcus Mutans* bacteria, cell viability (MTT assay) with 48 h and 10-days extracts, degree of conversion (DC), water sorption (WSO), and solubility (WSL), water contact angle (CA), flexural modulus (E), flexural strength (FS), compressive strength (CS), and Vickers microhardness (HV). The investigated materials have shown a complete reduction in bacteria adherence and satisfactory biocompatibility. The QA-PEI-NPs additive has no effect on the DC, VH, and E values. QA-PEI-NPs increased the CA (a favorable change), the WSO and WSL (unfavorable changes) and decreased flexural strength, and compressive strength (unfavorable changes). The changes mentioned were insignificant and acceptable for most composites, excluding the highest antibacterial filler content. Probably the reason for the deterioration of some properties was low compatibility between filler particles and the matrix; therefore, it is worth extending the research by surface modification of QA-PEI-NPs to achieve the optimum performance characteristics.

According to the latest data close to 39% of the world population have suffered from untreated dental caries in deciduous or permanent teeth and this percentage has increased extensively in the last 10 years^{1,2}. Furthermore, nearly 60% of adolescents and more than 90% of the adult population have experienced dental caries³—in the first stage of treatment most of them get dental fillings made of photopolymerizable resin-based composites. Their matrixes are based on a mixture of dimethacrylate monomers such as bisphenol A glycerolate dimethacrylate (Bis-GMA), ethoxylated bisphenol A dimethacrylate (Bis-EMA), triethylene glycol dimethacrylate (TEGDMA)

¹Faculty of Mechanical Engineering, Materials Research Laboratory, Silesian University of Technology, 18a Konarskiego Str., 41-100 Gliwice, Poland. ²Department of Physical Chemistry and Technology of Polymers, Silesian University of Technology, 9 M. Strzody Str., 44-100 Gliwice, Poland. ³Department of Microbiology and Immunology, Faculty of Medical Sciences in Zabrze, Medical University of Silesia in Katowice, 19 Jordana Str., 41-808 Zabrze, Poland. ✉email: grzegorz.chladek@polsl.pl

and/or urethane dimethacrylate (UDMA)⁴, which make it possible to develop materials characterized by advantageous functional features, including satisfactory aesthetic, physicochemical and mechanical properties^{5–7}.

The most frequent problem that causes the replacement of 57% to 88% of resin-based composite fillings is secondary caries^{8,9}. It is usually associated with the presence of a marginal gap induced primarily by polymerization shrinkage as well as the presence of porosities or other imperfections in the adaptation of material to tooth tissues^{10,11} with the simultaneous presence of pathogenic bacteria and products of their metabolism between restorations and teeth¹². It is also believed that bacterial adhesion with the biofilm accumulation that occurs on the surface of composite restorations is related to the initiation of secondary caries^{13,14}. Moreover, acid products of bacteria metabolism not only dissolve tooth minerals but may also lead to the degradation of composite restorations¹⁴. Another serious problem is the remaining caries caused by the imperfect removal of the tissues of infected teeth during treatment¹⁵. For these reasons, special attention has been focused on the development of new resin-composites with antibacterial properties to avoid colonization of the restorations' surface and/or the tooth-restoration interfaces by cariogenic bacteria^{16,17}. Different experimental strategies aimed at solving this problem have been considered. Antimicrobial agent release usually allows high local doses of antimicrobial agents to be obtained at specific sites and reduce the risk of systemic toxicity, but the durability of the effect is short and functional properties can often decrease. On the other hand, the contact-dependent strategy often has less or no adverse effects on mechanical properties, antibacterial activity is prolonged, but it is relatively weak with the risk of further reduction with surface biofouling¹⁷. In the last decade, much attention has been paid to dental composites enriched with antimicrobial nanoparticles and submicrometer-size particles such as silver¹⁸, zinc oxide¹⁹, cellulose nanocrystal/zinc oxide nanohybrids²⁰, zinc-doped mesoporous silica nanoparticles²¹, silver sodium hydrogen zirconium phosphate²², titanium dioxide²³ or chlorhexidine release systems^{24,25}. Some works suggest the use of essential oils²⁶. Other polymerizable compounds such as imidazole, chitosan loaded with dibasic calcium phosphate anhydrous, and chitosan particles show promising antimicrobial and biofunctional properties^{27,28}. These solutions are characterized by a different level of success in laboratory tests, and the most frequently reported problems include decreased aesthetic properties²⁹, cytotoxicity³⁰, and decreased mechanical properties^{31,32}.

Another nanomaterial considered as an antimicrobial filler for resin-based composites are cross-linked quaternary ammonium polyethylenimine nanoparticles (QA-PEI-NPs) in which the quaternary ammonium groups on the surface are responsible for antibacterial activity³³. The antimicrobial activity of QA-PEI-NPs against standard Gram-positive (such as *Staphylococcus aureus*) and Gram-negative (such as *Escherichia coli*) strains and numerous other pathogenic bacteria strains has been proven^{33–36}. It was also confirmed with diversified methodology that QA-PEI-NPs show activity against cariogenic bacteria *Streptococcus mutans* in in vitro tests^{37–40} and even against intraoral biofilm during an in vivo experiment⁴¹. However, little is known about other consequences of using QA-PEI-NPs as additives to resin-composite materials, because only in few studies modified commercially available resin-composite materials were investigated. Shvero et al.³⁸ show that 2% of QA-PEI-NPs do not change the degree of conversion of modified composites. Beyth et al.³⁹ introduced 1% (w/w) of QA-PEI-NPs into the flow and hybrid composite and registered a reduction in flexural strength (40%) for one of them. Beyth et al. and Yudovin-Farber et al.^{34,42} introduced up to 2 wt% of QA-PEI-NPs and reported no changes in cell viability after cytotoxicity tests. Barszczewska-Rybarek et al.⁴³ conducted more complex investigations, where up to 2 wt% of QA-PEI-NPs was introduced into the resin mixture of 60 wt% bis-GMA and 40 wt% TEGDMA (no reinforcing fillers were used). They registered an increase in water solubility and contact angle, a decrease in flexural strength (57%) and impact resistance, however, antimicrobial and cytotoxicity were not tested.

On the basis of the above, QA-PEI-NPs have been shown to be promising antibacterial additives for dental photopolymerizable resin-based composites. Research conducted so far mainly examined the microbiological properties of modified commercial materials, while the availability of tests of mechanical or physicochemical properties is very limited. Previous tests were also carried out with the use of QA-PEI-NPs concentrations not exceeding 2% (w/w). It is also interesting to find out whether and how the introduction of reinforcing fillers can change some unfavorable consequences observed in the case of the QA-PEI-NPs—resin matrix system. Moreover, no previous work has examined the influence of QA-PEI-NPs on the properties of the composites, at the same time taking into account the biological, physicochemical, and mechanical properties, because in each of the available studies other commercially available composites were modified as starting material. As a result, the research conducted so far cannot be considered as a coherent whole for methodological reasons. In order to gain additional knowledge it is therefore necessary to conduct tests with the use of experimental model composite materials with a precisely known composition with a wider range of QA-PEI-NP concentrations. This article aims to provide for the lack of knowledge about the property relationships of dental dimethacrylate polymer-based composites enriched with QA-PEI-NPs. The research hypothesis was that QA-PEI-NPs introduction into experimental composites considered as dental restorative materials allows to obtain a reduction of adhered cariogenic bacteria on surfaces while maintaining the desired biofunctional properties. The null hypothesis was that the introduction of QA-PEI-NPs would not affect the mentioned properties of experimental composites.

Materials and methods

Synthesis of QA-PEI-NPs

The QA-PEI-NPs were synthesized with the method described by by Yudovin-Farber et al.⁴⁴ with additional specifications described in details by Barszczewska-Rybarek⁴³. The poly(2-ethyl-2-oxazoline) (PEtOx) (Sigma Aldrich, St. Louis, MO, USA) was dissolved in distilled water in a flask equipped with a magnetic stirrer, thermometer and condenser. Aqueous solution of hydrochloric acid (37 wt%, Acros Organics, Geel, Belgium) was added, and the reaction mixture was refluxed with the use of the oil bath. The mixture was cooled (room temperature) and unreacted hydrochloric acid and formed propionic acid were removed under reduced pressure.

The residue acid was neutralized with sodium hydroxide (Chempur, Piekary Śl., Poland) solution in distilled water to pH 9–10. The obtained white PEI was recrystallized from distilled water, dissolved in methyl alcohol, purified by precipitating into ice-cooled diethyl ether, next filtrated and finally dried under reduced pressure. The solution of the obtained PEI in anhydrous ethanol (Stanlab, Lublin, Poland) was introduced into a flask equipped as previously described, the 1,5-dibromopentane (Acros Organics, Geel, Belgium) was introduced and the reaction was refluxed for 24 h. Next, the 1-bromooctane (Acros Organics, Geel, Belgium) was introduced and the mixture was refluxed again for 24 h and hydrobromic acid was neutralized with sodium bicarbonate (Chempur, Piekary Śl., Poland). For quaternization reaction the mixture was refluxed for 48 h after adding iodomethane and the resulting hydroiodic acid was neutralized with sodium bicarbonate under reflux. The obtained QA-PEI-NPs were purified by precipitation in distilled water, washing several times with hexane (Chempur, Piekary Śl., Poland) and distilled water, centrifuged, and finally lyophilized to dryness.

Composite preparation

The matrix consisted of bisphenol A glycidyl methacrylate (bis-GMA), urethane-dimethacrylate (UDMA), and triethylene glycol dimethacrylate (TEGDMA) mixed at a weight ratio of 40:40:20, respectively, 0.4% (w/w) of camphorquinone as the photosensitizer, and 1% (w/w) of N,N-dimethylaminoethyl methacrylate (DMAEMA) as a photoaccelerator (all ingredients purchased from Sigma-Aldrich, St. Louis, MO, USA). The reinforcing fillers were two types of silanized barium borosilicate glass with a mean particle size of 2 μm (Schott AG, Landshut, Germany) and 0.7 μm (Esschem, Linwood, PA, USA) used at a weight ratio of 65:35, respectively.

The QA-PEI-NP nanoparticles were compounded at concentrations of 0.5, 1, 1.5, 2, 3% (w/w), and the masses necessary to prepare the composites were calculated according to the equation:

$$m_{\text{QA-PEI-NP}} = \frac{c_{\text{QA-PEI-NP}} \times m_c}{1 - c_{\text{QA-PEI-NP}}} \quad (1)$$

where $m_{\text{QA-PEI-NP}}$ was the QA-PEI-NPs mass, g; $c_{\text{QA-PEI-NP}}$ was the QA-PEI-NPs concentration, % (w/w); m_c was the matrix with glass fillers mass (constant), g.

The fillers were compounded in 50 mL glass beakers at room temperature in a darkroom equipped with a red LED lamp. All composites were prepared based on a 35 g portion of the matrix, and reinforcing fillers. The compounding was carried out gradually in standard portions of maximum 0.25 g of fillers (smaller for the 0.5% of QA-PEI-NPs or for the last portions of fillers) in the following order: QA-PEI-NPs, 0.7 μm glass, and 2 μm glass. Compounding was achieved by multiple, subsequent spreading and mixing of composition. The compounding process for a 35 g portion of composite took approximately 2 h to 2.5 h—longer time was required for higher concentrations due to increased viscosity. The prepared materials were placed under the pressure of 80 mbar for 2 h in a modified vacuum stirrer (Twister evolution, Renfert, Germany) to remove air bubbles created during compounding and finally were transferred to dark pharmacy jars, where they have been safely stored.

Photopolymerizations were carried out in teflon disc-like molds (degree of conversion (DC), compressive strength (CS), Vickers microhardness (HV)) and stainless steel molds (microbiological tests, water sorption (WSO), and solubility (WSL), water contact angle (CA), flexural modulus (E), flexural strength (FS)). The mold was placed on a microscope slide, material was packed in the mold, covered with 50 μm thick polyester foil and another microscope slide, that was pressed for 1 min to remove excess material. All samples were irradiated between two 50 W LED panels, each measuring 25 mm × 25 mm and equipped with 50 BRIDGELUX 45mil diodes characterized with optical wave length 440–450 nm (Fremont, USA). Irradiation time was 40 s at room temperature. After polymerization slides and foil were taken away, excess material was removed, samples were pushed out of molds, rinsed with distilled water and stored in distilled water in dark conditions at 37 °C for 24 h.

The experimental composite without the addition of QA-PEI-NPs was used as a control material, but to compare its microbiological properties with commercially available products, additional tests using Arkona Boston (AB) composite (Arkona Laboratory of Dental Pharmacology, Poland) were prepared. AB is composed of bis GMA, TEGDMA, UDMA, bis EMA, fillers measuring from 20 nm to 2 μm (barium borosilicate glass and silica) and CQ:DMAEMA photoactivating system.

Due to the influence of surface roughness on the results of microbiological tests (adherence of bacteria and cell viability assay), these samples were wet-ground with P500-grit abrasive paper to standardize the surface and rinsed with distilled water. The goal was to obtain comparable surface finishing with was controlled (Ra) with a Surtronic 25 contact profilometer (Taylor-Hobson, UK). On each surface (top and bottom), 3 measurements were made (radially), and the mean value was taken as the roughness value for sample⁴⁵. The length of the measurement path was 0.8 mm and the range was 10 μm. The results were then subjected to statistical analyses to confirm that there were no significant differences between the groups.

Adherence of bacteria

Bacterial adhesion tests were performed by incubating 10 mm × 1.5 mm (diameter × thickness) disc-shaped samples. Surfaces of all samples were wet-ground with P500-grit abrasive paper. All samples were placed for 18 h in 1 mL of *Streptococcus mutans* ATCC 33535 bacterial suspension ~ 5 × 10⁶ CFU/mL (CFU—colony forming units) at 37 °C. The samples were cleaned with sterile water and vortexed (1 min, 3000 rpm) in 1 mL of sterile water, 100 μL of the bacteria suspensions were serially diluted with 0.9% NaCl. 100 μL of these solutions and 100 μL of undiluted bacteria suspensions were seeded onto Columbia agar (bioMerieux, Marcy l'Etoile, France) with 5% sheep blood plates. The cultured plates were finally incubated at 37 °C for 24 h, and the number of bacteria that adhered to the surfaces was determined by counting the colonies.

Cell viability assay (MTT assay)

Obtaining extracts of tested composites

Extracts of the tested composites were obtained according to the procedure in accordance with the EN ISO 10993-5:2009 standard. Samples of each of the materials tested were placed individually in the wells of a 24-well plate in a volume of 2 mL of culture medium identical in its composition to the medium used for the culture of fibroblasts of the L-929 line used in further studies. The prepared plates were incubated at 37 °C in an atmosphere of 5% CO₂ for 2 or 10 days, thus obtaining 2-day and 10-day extracts. Under the same conditions as for the composite samples, the culture medium itself was also incubated in the wells of the plate as controls. Extracts and control media collected after incubation were stored at – 80 °C until tests were performed to assess the viability of L-929 cells.

Cell culture of the L-929 line

In vitro studies, mouse fibroblasts from the L-929 line (NCTC clone 929) purchased from the American Type Culture Collection (Manassas, VA, USA) were used. Cell line L-929 (ATCC, catalog number CCL-1) consisted of subcutaneous connective tissue fibroblasts of mice of the C3H/An strain. ATCC formulated Eagle's Minimum Essential Medium (EMEM) with 10% horse serum penicillin (100 IU/mL), and streptomycin (100 µg/mL) was used for L-929 cells. Cell culture was carried out in 25 cm² polystyrene flasks for the cultivation of adherent cells (Nunc EasYFlasks™ Nunclon™ Delta from Nunc A/S, Roskilde, Denmark). Cells were continuously grown in an MCO-17 AIC incubator from Sanyo (Japan), providing constant culture conditions (37 °C, 5% CO₂ atmosphere at 100% relative humidity). Cells were passaged at 2–3 day intervals. For experimental studies, a suspension with a final density of 1 × 10⁵ cells/mL of medium was used. The density of the cell suspension was assessed by microscopy using a Burkner chamber.

Evaluation of the viability of L-929 cells contacted with the extracts of the tested composites

The cytotoxicity assessment of the tested composites was carried out according to the recommendations of the EN ISO 10993-5 standard⁴⁶. Model L-929 cells (mouse fibroblasts) under in vitro culture conditions were contacted for 24 h with undiluted extracts. After 24 h of incubation, cell viability was assessed using the bromo-3-[4,5-dimethylthiazol-2-yl]-2,5-diphenyltetrazolium assay (MTT assay). In this test, the measurement of mitochondrial dehydrogenase activity made it possible to determine the percentage of live cells in cultures contacted with a specific extract, and thus to determine the cytotoxicity of the tested composites. According to the recommendations of the EN ISO 10993-5 standard, a reduction in the viability of cells contacted with the extracts tested by more than 30% as compared to the control cell culture (viability below 70%) was considered a cytotoxic effect.

Well of a 96-well microplate were dispensed with 100 µL of L-929 cell suspension at a density of 1 × 10⁵ cells/mL (10,000 cells/well) in RPMI 1640 medium with 10% FBS, penicillin (100 IU/mL) and streptomycin (100 µg/mL). After 24 h of incubation at 37 °C in an atmosphere containing 5% CO₂ and 100% relative humidity, the supernatants were removed and 100 µL of undiluted extract of a specific test preparation or medium after incubation conducted in parallel with obtaining extracts. The control culture consisted of cells contacted with fresh culture medium. After 24 h of incubation at 37 °C in an atmosphere of 5% CO₂ and 100% relative humidity, MTT solution at a final concentration of 1.1 mM in fresh culture medium was dispensed into each well after removal of the culture medium. After 3 h of incubation at 37 °C in 5% CO₂ at constant relative humidity, the supernatants were removed and 200 µL of DMSO was added to the test and control cultures to extract MTT formazan. After 20 min, 150 µL of the solution was taken from each well and its absorbance was determined at 550 nm using the Eon automatic plate reader (BioTek Instruments, Winooski, VT, USA). The intensity of the violet color of the solution was directly proportional to the amount of formazan formed and thus the number of viable cells.

Cell viability (%) was calculated using the following formula:

$$\text{Cell viability} = \frac{A_b}{A_k} \times 100\% \quad (2)$$

where: A_b —the absorbance of the test sample, A_k —the absorbance of the control.

Degree of conversion

The DC was determined from the spectra obtained with the Fourier Transform Infrared Spectrometer (Spectrum Two, Perkin-Elmer, Waltham, MA, USA). Samples were analyzed in the form of KBr pellets with 128 scans at a resolution of 1 cm⁻¹. The DC was calculated from the decrease of absorption band at 1637 cm⁻¹ referring to the C=C stretching vibration ($A_{C=C}$), in relation to the peak at 1608 cm⁻¹, assigned to the aromatic stretching vibrations (A_{Ar}) with the following equation⁴⁷:

$$DC(\%) = 1 - \frac{\left(\frac{A_{C=C}}{A_{Ar}}\right)_{\text{after polymerization}}}{\left(\frac{A_{C=C}}{A_{Ar}}\right)_{\text{before polymerization}}} \times 100\% \quad (3)$$

Vickers hardness

Five cylindrical samples (6 mm in diameter and 3 mm in height) were prepared from each composite. Five indentations were made on each sample, and average values are denoted as hardness. Measurements were made at a 0.4905 N (0.05 kgf) load and a loading time of 15 s⁴⁸ (Future-Tech FM-700 microhardness tester, Future-Tech

Corp, Tokyo, Japan) and Vickers hardness was calculated automatically based on the average length of the diagonal left by the indenter.

Compressive strength

Ten cylindrical samples (4 mm in diameter and 8 mm in height) were prepared from each composite, but according to the recommendation of Galvão et al.⁴⁹ they were additionally light-irradiated on lateral surfaces after being removed from molds. The tests were carried out with a cross head speed of 0.5 mm/min at a universal testing machine (Zwick Z020 GmbH & Com, Ulm, Germany), and the CS values were calculated according to the equation:

$$CS = \frac{F}{A} \quad (4)$$

where: CS—the compressive strength, MPa; F—force at fracture, N; A—the initial cross-sectional area, mm².

Flexural strength

Three-point bending tests were carried out using a universal testing machine in accordance with the ISO 4049 standard⁵⁰. Ten bar samples 25 mm × 2 mm × 2 mm (length × width × thickness) were prepared from each material. The cross-head speed was 0.75 mm/min and the distance between the supports was 20 mm. FS strength and E were calculated with the following formulas:

$$FS = \frac{3Pl}{2bh^2} \quad (5)$$

$$E = \frac{P_1 l^3}{4bh^3 \delta} \quad (6)$$

where: l—the distance between the supports, mm; b and h—the width and height, mm; P—the maximal force, N; P₁—the load at the chosen point at the elastic region of the stress–strain plot, kN; δ—the deflection in P₁.

Sorption and solubility

The test was carried out according to ISO 4049⁵⁰. Five samples of each material (measuring 15 mm in diameter and 1 mm in height) were dried inside desiccators with freshly dried silica gel at 37 ± 1 °C and weighed daily (Analytic Scale AS 60/220.X2.PLUS, Radwag, Poland) with an accuracy of 0.1 mg to achieve a constant value of the mass m₁ (daily changes < 0.1 mg). Samples were placed separately in 10 mL of distilled water for 7 days at 37 ± 1 °C and rapidly dried from visible moisture with filter paper, m₂ mass values were registered, and the drying was repeated to constant mass registers as m₃. The WSO and the WSL were calculated according to the following formulas:

$$WSO = \frac{m_2 - m_3}{V} \quad (7)$$

$$WSL = \frac{m_1 - m_3}{V} \quad (8)$$

where, m₁—the initial mass of the dried sample, µg; m₂—the mass after storing, µg, m₃—the mass after the second drying, µg; and V—the volume of the sample after the first drying, mm³.

Water contact angle

The five polymerized composites were tested for water contact angle (CA) using a goniometer (OCA 15EC, Data Physics, Filderstadt, Germany). Deionized water (4 µL) was dropped onto the tested surface via the sessile drop method.

Statistical analysis

Statistical analysis was performed using the PQStat ver. 1.6.6.204 (PQStat Software, Poland). The residuals distributions were tested with Shapiro–Wilk, the equality of variances was tested with the Levene test and one-way ANOVA with a possible F * correction (Brown-Forsythe) and Tukey HSD post hoc tests were used (for all tests α = 0.05). The results of microbiological tests were statistically evaluated using non-parametric Kruskal–Wallis test (α = 0.05) with Dunn–Bonferroni post hoc test and Mann–Whitney U test.

Results

The number of live *S. mutans* bacteria adhered to the surfaces decreased significantly (p < 0.0001) after the introduction of QA-PEI-NPs (Table 1, Fig. 1). For composites with QA-PEI-NPs no adhered bacteria were observed, for control composite material the average value was 17.03 × 10² CFU/mL while for the commercial composite (AB) the average value was 11.56 × 10² CFU/mL and the registered differences were not statistically significant (Supplementary Table 1).

The mean viability values of L-929 cells for the extracts of the tested materials are presented in Table 1 and Fig. 2 (the detailed results are summarized in Supplementary Table 2). For 2-day extracts, there was no

$c_{QA-PEI-NP}$ %	Number of adhered bacteria, $\times 10^2$ CFU/ mL		Viability of L-929 cells, %			
	(p < 0.0001)		2 days (p = 0.2795)		10 days (p = 0.0145)	
	AV	SD	AV	SD	AV	SD
0 (control)	17.03 ^a	3.23	89.6	3.6	91.1 ^a	3.2
0.5	No adhered bacteria ^b		91.0	5.5	84.7 ^{a,b}	2.2
1	No adhered bacteria ^b		88.7	3.3	87.7 ^{a,b}	3.1
1.5	No adhered bacteria ^b		87.0	2.0	82.1 ^{a,b}	1.9
2	No adhered bacteria ^b		86.7	1.2	83.4 ^{a,b}	3.8
3	No adhered bacteria ^b		82.2	5.2	78.5 ^b	3.7

Table 1. The number of *S. mutans* bacteria adhered to composites' surface and viability of L-929 cells after 24 h of incubation with the 2-days and 10 days extracts. The different lowercase letters (a–b) for column show significantly different results at the level of $p \leq 0.05$. AV average value, SD standard deviation, CFU colony forming units.

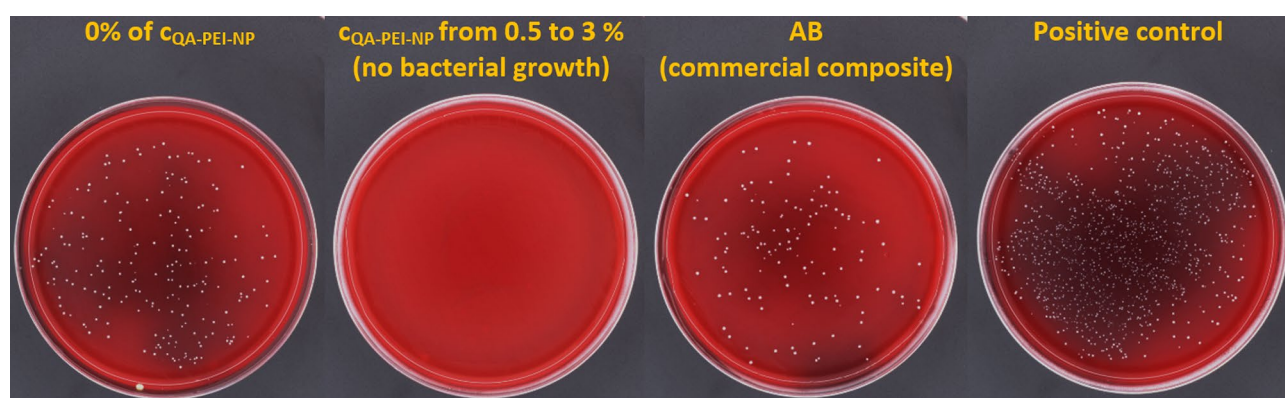


Figure 1. Representative images presenting the results of the *Streptococcus mutans* ATCC 33535 adherence test—cultured plates after incubation with undiluted bacteria suspensions.

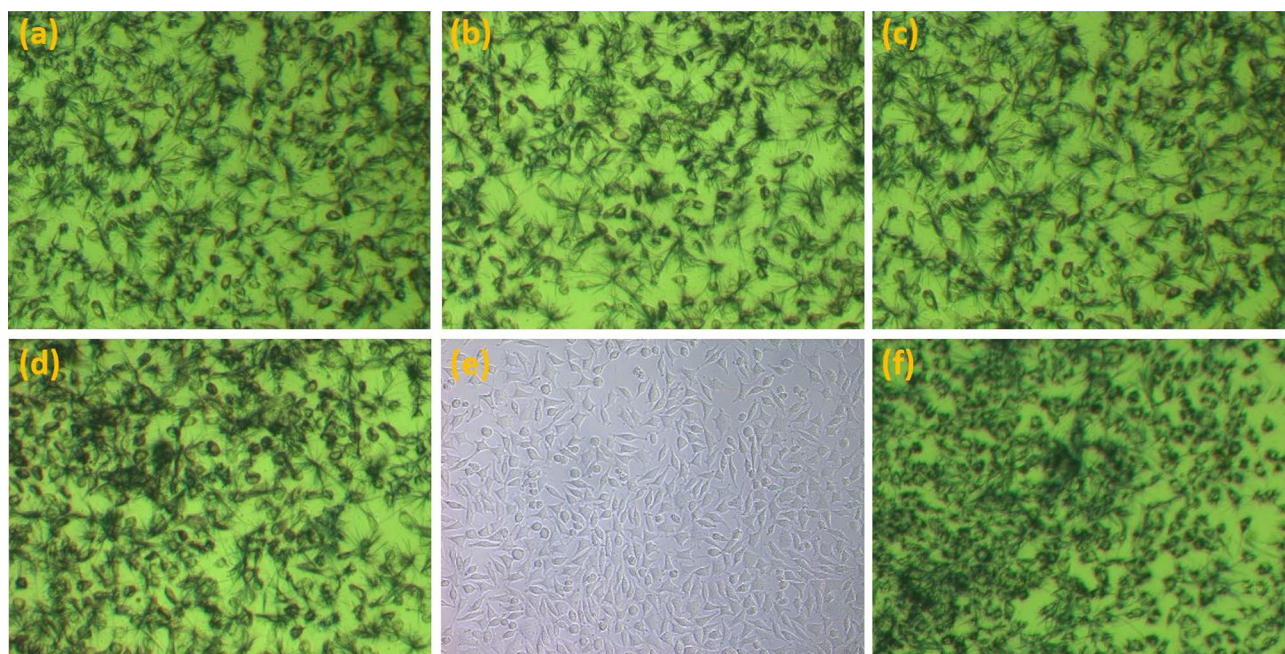


Figure 2. Representative images of L-929 line cells after 24 h incubation with undiluted 2 days (a) and 10 days (b) extracts of the experimental control composite (0% of QA-PEI-NP) after MTT assay, 2 days (c) and 10 days (d) extracts of the experimental composite containing 3% of QA-PEI-NP after MTT assay, control culture of adhered L-929 cells before MTT test (e) and control culture of adhered L-929 cells after MTT test (f).

statistically significant difference ($p = 0.2795$) between the results obtained for the control composite (89.6%) and the experimental composites, however, for 3% QA-PEI-NPs the average viability value was lower than for other materials (82.2%). For 10 days, the extracts showed a statistically significant decrease ($p = 0.0145$) in viability and the post hoc test confirmed that compared to control material (cell viability was 91.1%) cell viability decreased for 3% QA-PEI-NPs ($p = 0.0118$) for which the lowest value was observed (78.5%). The reduction in viability of L-929 cells due to the extension of the time to obtain the extract was registered for materials enriched with QA-PEI-NPs; however, it was not statistically significant ($p > 0.05$). An additional experiment (Supplementary Table 3) confirmed that there were no statistically significant differences in cell viability for the control composite and the commercially available product. Representative microscopic images of L-929 cells obtained for the experimental preparation compared to control cultures of adhered L-929 cells are presented in Fig. 3.

The HV of composites ranged from 47.4 HV0.05 to 50.3 HV0.05 and there were no statistically significant differences ($p = 0.052$) between average values (Table 2).

The composites' CS ranged from 219.5 MPa to 317.7 MPa (Table 2) and a statistically significant ($p < 0.0001$) decrease came with increasing QA-PEI-NPs concentrations. For composites with QA-PEI-NPs concentrations starting from 1% the CS values were significantly lower than for the control material (from $p = 0.0001$), however, there were no significant differences between materials enriched with 1.5% to 2% and 2% to 3% QA-PEI-NPs ($p > 0.05$).

The FS of composites ranged from 78.0 MPa to 100.1 MPa (Table 2) and decreased statistically significantly ($p < 0.0001$) with the increasing QA-PEI-NPs content. Statistically significant decreases were registered for composites enriched with 2% ($p = 0.0008$) and 3% ($p = 0.0002$) of QA-PEI-NPs. The E values ranged from 7.3 to 7.8 GPa and there were no statistically significant ($p = 0.169$) differences between the average values.

The DC of composites ranged from 59.8% to 64.2% and there were no statistically significant ($p = 0.9451$) differences between average values (Table 3).

The composites' WSO ranged from 20.0 $\mu\text{g}/\text{mm}^3$ to 25.1 $\mu\text{g}/\text{mm}^3$ and increased with the increasing QA-PEI-NPs content ($p < 0.0001$) (Table 3). Statistically significant differences in comparison to control material were registered for the concentration of 1.5% QA-PEI-NPs ($p = 0.0019$, 18% increase), 2% QA-PEI-NPs ($p = 0.001$, 18% increase), and for the highest content ($p = 0.0001$, the increase was 25%). For most of the experimental composites the average WSO values did not differ statistically significantly, but statistically significant differences were registered for 3% QA-PEI-NPs in comparison to 0.5 QA-PEI-NPs ($p = 0.0119$) and 1 QA-PEI-NPs ($p = 0.0223$). The composites' WSL ranged from 2.6 $\mu\text{g}/\text{mm}^3$ to 5.6 $\mu\text{g}/\text{mm}^3$. The increasing QA-PEI-NP content caused a gradual increase in WSL values ($p = 0.0017$), however, differences were statistically significant only for the highest QA-PEI-NP concentration where there was an abrupt increase of 119% compared to the control

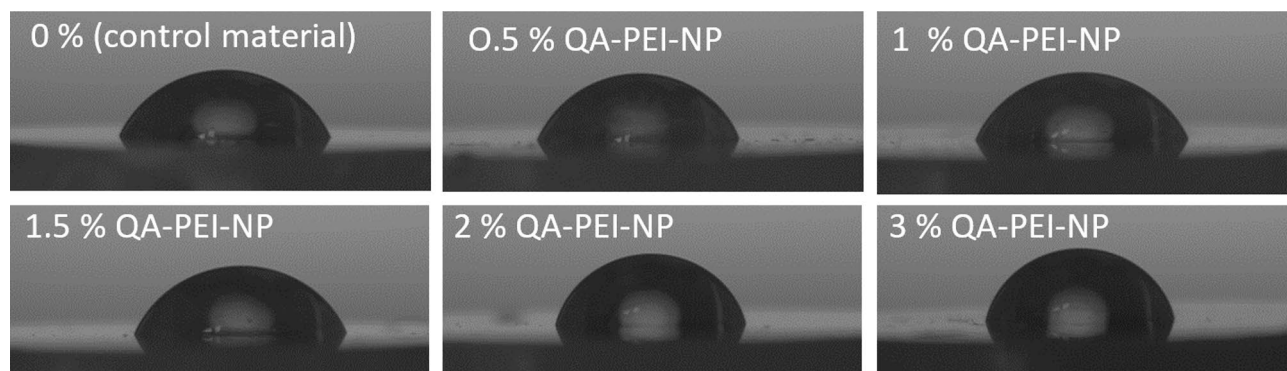


Figure 3. Representative images of deionized water droplets on the composite surfaces obtained from the goniometry camera.

$c_{\text{QA-PEI-NPs}} \%$	HV0.05		CS, MPa		FS, MPa		E, GPa	
	(p = 0.052)		(p < 0.0001)		(p = 0.0001)		(p = 0.169)	
	AV	SD	AV	SD	AV	SD	AV	SD
0	48.8	0.8	317.7 ^a	13.1	100.1 ^a	8.7	7.3	0.4
0.5	48.7	1.3	309.9 ^a	9.6	91.8 ^a	13.3	7.6	0.5
1	49.3	1.1	273.6 ^c	9.2	90.9 ^a	11.9	7.8	0.5
1.5	48.6	0.8	250.5 ^{c,d}	20.2	89.4 ^a	3.8	7.7	0.5
2	50.3	1.6	234.0 ^{d,e}	20.5	85.3 ^b	7.7	7.6	0.7
3	47.4	1.1	219.5 ^c	14.3	78.0 ^b	8.2	7.4	0.5

Table 2. Vickers hardness, compressive strength, flexural strength and flexural modulus after the introduction of QA-PEI-NPs. The different lowercase letters (a–e) for a column show significantly different results at the level of $p \leq 0.05$. AV average value, SD standard deviation.

$c_{QA-PEI-NP}$ %	DC, %		WSO, $\mu\text{g}/\text{mm}^3$		WSL, $\mu\text{g}/\text{mm}^3$		CA, °	
	(p = 0.9451)		(p < 0.0001)		(p = 0.002)		(p = 0.0017)	
	AV	SD	AV	SD	AV	SD	AV	SD
0	63.6	8.9	20.0 ^a	1.2	2.6 ^a	0.2	73.0 ^a	1.8
0.5	64.2	7.4	22.0 ^{a,b}	2.2	3.7 ^a	0.7	72.8 ^a	1.2
1	61.3	5.8	22.3 ^{a,b}	0.3	3.7 ^a	0.6	73.4 ^a	2.1
1.5	60.1	9.0	23.7 ^{b,c}	0.6	4.0 ^{a,b}	0.6	74.5 ^{a,b}	1.8
2	59.8	8.8	23.9 ^{b,c}	0.9	3.9 ^{a,b}	0.3	76.6 ^{a,b}	2.2
3	60.9	4.8	25.1 ^c	0.9	5.6 ^b	1.7	77.9 ^b	1.6

Table 3. The degree of conversion, water contact angle, sorption and solubility of composites after the introduction of QA-PEI-NPs. * The different lowercase letters (a–c) for column show significantly different results at the level of $p \leq 0.05$. AV average value, SD standard deviation.

material. The statistically significant differences were registered for the control material, 0.5% QA-PEI-NPs and 1% QA-PEI-NPs vs. 3% QA-PEI-NPs ($p = 0.0006$, $p = 0.0364$, $p = 0.465$, respectively).

The composites' CA ranged from 73.0° to 77.9°. Increasing QA-PEI-NP concentration caused a gradual increase in CA values ($p = 0.0017$). Differences were statistically significant for the highest QA-PEI-NP concentration and control material ($p = 0.0088$, the increase was 7%), 0.5% QA-PEI-NPs ($p = 0.0059$) and 1% QA-PEI-NPs ($p = 0.02$) composites.

Discussion

The development of antibacterial resin-based composites is one of the most important pathways of investigations regarding direct dental filling materials. In this study, QA-PEI-NPs synthesized with the previously described method^{43,51} and characterized by an average size of 151 nm which was reported as optimal⁴³ were introduced into a representative bis-GMA-TEGDAM-UDMA matrix, finally compounded with two glass reinforcing fillers⁵².

The antimicrobial action of QA-PEI-NPs against cariogenic bacteria was recorded in previous in vitro studies. Beyth et al.³⁹ and Shvero et al.³⁸ found that commercially available flow and hybrid composites modified with 1% of QA-PEI-NPs present durable antibacterial activity against *S. mutans* in a direct contact test and strong activity during 24 h contact confirmed by SEM investigations. Similar results were obtained with an analogous methodology for additional modified commercial composites^{37,40}. In these investigations, only formulations that contained 1% and 2% were tested. In our study, strong antibacterial activity against *S. mutans* was also confirmed for a lower concentration (0.5%) with another methodology, because the current experiment was based on the adherence of bacteria cells to the samples' surfaces. Due to the nature of the test, attention was paid to the finishing of the samples' surface, because roughness is related to bacterial adherence to the composites^{53,54}. All samples were ground which selected abrasive sandpaper which gave a roughness measured during quality control of ~0.35 μm (from 0.27 to 0.4 μm) which corresponds to the typical values after finishing the fillings under clinical conditions, that range from 0.1 μm to 0.6 μm (usually from 0.25 μm to 0.4 μm)^{55–59}. The antibacterial action of the used NPs is related to the properties of positively charged quaternary ammonium groups of QA-PEI, which interact with negatively charged bacterial cell walls disrupting its electrical balance, which finally leads to a decrease in its osmoregulatory and physiological roles of the membrane resulting in cell death⁶⁰. Introducing this polymeric additive in the form of NPs is advantageous, because of its specific surface being exceptionally large, so low concentrations can be used to achieve antimicrobial activity⁶¹. However, the condition for success is to obtain a homogeneous distribution of the antimicrobial filler⁶² that should be close to 1 NP/ μm^2 to ensure its contact leading to activity against bacteria³⁸. Our research has shown that at a concentration of QA-PEI-NPs lower than previously used, it is still possible to achieve a sufficient distribution of particles to prevent cariogenic bacteria cells from surviving on the surface. Some limitation indicating the need for caution in interpreting the results may be the fact that adsorption of saliva ingredients to the surface and the creation of biofilms on the fillings may potentially cover the antibacterial groups of QA-PEI-NPs, regardless of the results of an in vivo experiment which suggests, that after 4 h of biofilm creation, the antibacterial action is still effective⁴¹.

Biocompatibility tests showed that cell viability for incubation times exceeded 70%, so none of the materials showed cytotoxic properties after two as well as after ten days of extraction⁴⁶. Furthermore, there were no differences in cell viability after two days of incubation for all materials, which stay consistent with previous cytotoxicity investigations conducted with different methodologies and cell lines for composites with up to 2% of QA-PEI-NPs^{34,42}. After a ten-day extraction of the samples containing the highest concentration, a decrease of 14% in cell viability was observed compared to the control material. Other studies reported that QA-PEI-NP suspensions reduced cell viability in cytotoxicity assay, but cytotoxicity occurred only at concentrations a few times higher than necessary to obtain an antibacterial effect⁶³. This stays in accordance with our results. Yudovin-Farber et al.⁴⁴ suggested that the reduction of cell viability in the cytotoxicity test against mammalian cells caused by QA-PEI-NPs is related to a strong positive charge of the nanoparticles, so its action is analogous to the one previously described for prokaryotic cells. However, it is emphasized that the mechanism of binding to cell walls causing membrane disruption through direct interactions or through reactive oxygen species production is much less toxic in mammalian cells than in bacteria, because the first ones may phagocytize NPs, and degrade them by lysosomal fusion to a certain degree with finally reduced toxicity^{63,64}. This may be the reason why, even

after a longer than typical time of obtaining extracts, the reduction of fibroblast cell viability even for the highest concentration of QA-PEI NPs associated with their presence on the surface and/or their leaching was still small.

The degree of conversion of double bonds is an important feature of dental composites based on dimethacrylate monomers due to the potential risk of biological responses of pulp tissue related to the release of monomers⁶⁵ as well as the influence on mechanical and physicochemical properties⁶⁶. Our results are in agreement with the earlier findings, where 2% of the QA-PEI-NPs did not significantly change the DC values of the modified commercial composites³⁸ and the Bis-GMA/TEGDMA matrix⁴³. The DC values were also typical for formulations based on similar dimethacrylate systems⁶⁷. As light passes through the solid material with increasing density, such as a filled composite, its intensity decreases⁶⁸. Moreover, the composite ingredients such as fillers scatter and absorb light more effectively than the matrix, decreasing the power density with distance from the sample surface and finally decreasing the DC values⁶⁹. Increased scattering in the composites also occurs when filler particle size is from one-half to close to that of the curing light wavelength⁷⁰. Our earlier work related to the characterization of the QA-PEI-NPs showed only a small percentage of particles of this size in the synthesized powder⁴³ and the concentrations of QA-PEI-NPs were low (max. 3%) in comparison to those of other fillers content, so their influence on the additional scattering or absorption of light was not sufficient to affect significantly the DC of composites. It cannot be ruled out that an increase in the content of QA-PEI-NPs could lead to such changes. The potential reduction in DC after introducing new antimicrobial fillers has been recognized to be correlated with decrease in microhardness^{22,71}, which is consistent with our research, as both the DC and hardness values did not change significantly. In this context, microhardness measurements confirm the preservation of beneficial properties of the polymer matrix. On the other hand, the introduction of ceramic fillers usually increases the hardness due to their characteristics and the high interfacial shear strength between the nanofiller and the resin matrix, which increased the resistance to localized plastic deformation⁷². However, the nanoparticles used in this work, due to the comparable hardness of antimicrobial polymers and typical polymeric matrixes of dental composites^{73,74} cannot lead to an increase in hardness. In this context, the results achieved were favorable. In addition, stable microhardness values should be considered beneficial because a reduction in hardness can lead to increased wear^{75,76} and swallowing more friction products with chewed food and saliva.

Three mechanical properties on the macroscale were analyzed, the compressive, flexural strength, and flexural modulus. Compressive forces are generated during mastication, especially when composite fillings replace a large volume of tooth tissues⁷⁷, while flexural forces are particularly important in stress-bearing cavities for restoration classes I, II, and IV⁷⁸. The decrease in CS values was significant for materials enriched with QA-PEI-NP excluding one that contained 0.5% filler; however, for concentrations of 1% it was 14%, while for 3% it was 31%. The recommended values of CS are comparable with the plastic limit of tooth tissues^{49,79}, whose average values are up to 170 MPa for dentine and up to 225 MPa for enamel⁸⁰. This indicates that up to 1.5% of QA-PEI-NP CS values were fully satisfactory, but starting from 2% they may not allow the full use of the load-bearing capacity of tooth tissues in some cases. The effect of QA-PEI-NPs on CS composites was not investigated in the past; however, the introduction of metallic or ceramic antibacterial particles gives diversified results, from no effect even at high contents for cubic-shaped silver-enriched ceramic particles²² to increasing at low and decreasing at higher concentrations of metallic and ceramic NPs^{81–83}. FS values systematically decreased with increasing concentration of QA-PEI-NP; however, statistically significant reductions of 15% and 22% were recorded for 2% and 3%, respectively. For the highest content of QA-PEI-NP, the registered values were below the limit of 80 MPa recommended by the ISO 4049 standard for restorations of the occlusal surfaces⁵⁰. Beyth et al.³⁹ reported that 1% of QA-PEI-NP resulted in a reduction in FS by approximately 40% for a composite based on the bis-GMA/TEGDMA matrix and 47% of reinforcing fillers, but do not have a significant influence on the commercial material based on the bis-GMA/UDMA/TEGDMA matrix reinforced with 60% fillers. Barszczewska-Rybarek et al.⁴³ also reported a significant reduction of FS values (up to 57%) for Bis-GMA/TEGDMA resin after introducing 0.5% to 2% of QA-PEI-NPs. After considering their own and Beyth et al.³⁹ results, the authors suggested that matrixes containing UDMA due to participation in strong hydrogen bonding may allow one to create formulations that are less sensitive to flexural stress after introducing new particles. Our results support this concept because decrease in FS was not significant up to 1.5% of QA-PEI-NPs. However, it does not explain still large FS and CS changes at relatively low concentrations of QA-PEI-NPs, because numerous types of particles with antimicrobial properties introduced into similar matrixes do not degrade mechanical properties at such content. Stencil et al.²² showed a reduction in FS after compounding a 16% cubic-shaped ceramic filler, Tavassoli Hojati et al.⁸³ introduced up to 5% of ZnO-NPs into a bis-GMA/UDMA/TEGDMA-based composite, while Brandão et al.⁷¹ compounded up to 10% of ZnO-NPs into a bis-GMA/TEGDMA-based material, and both did not register significant changes in FS. The reduction of the mechanical properties on a macroscale after using QA-PEI-NPs even at low concentrations may suggest weak compatibility of QA-PEI-NPs with the resin phase, which results from poor wettability of particles by matrix components and/or adhesion of phases. Weak interactions between these ingredients may result in creation of voids around the particles, which are structural defects. They may expand when a load is applied and act as stress concentrators, leading to a decrease in CS and FS. This shows that further investigations should take into account physical or chemical surface modifications of QA-PEI-NPs to eliminate this problem⁸⁴.

The clinically acceptable values of the flexural modulus can vary, with a relatively lower modulus to flex with the teeth for cervical cavities or higher to withstand the occlusal forces for posterior composites⁸⁵. The E values of the composites studied did not change significantly due to the addition of QA-PEI-NPs, which remain in accordance with previous reports^{39,43} and can be considered an advantage because it indicates that there were no significant changes in the molecular structure of the polymer network such as an increase in the loop number that could cause a decrease in E values without a decrease in the DC⁶⁶.

Water sorption and solubility are other key physicochemical properties of dental composites due to their potential influence on biocompatibility related to the washout of ingredients and being often associated with

the stability of dimensions or mechanical properties caused by liquid uptake⁸⁶. The registered WSO values for all samples were lower than 40 $\mu\text{g}/\text{mm}^3$, however WSL values for 2 samples with 3% of QA-PEI-NPs exceeded 7.5 $\mu\text{g}/\text{mm}^3$, so these materials did not meet the requirements of the ISO standard⁵⁰. The increase in WSO/WSL has been reported for materials containing nanoparticles^{69,87}, including QA-PEI-NPs⁴³. Matrix properties such as a decrease in DC are often mentioned in the context of the relationship with the increase in WSO/WSL^{88,89}, however in this study no differences in DC were observed, which suggest another cause of changes. Increased WSO and WSL can be another factor indicating low compatibility between filler particles and the matrix, because water can migrate and accumulate at the matrix-filler particles and/or their aggregation interface, which may explain especially larger changes for higher filler concentrations^{7,22}. Large surface area, typical for the NPs, may also favor degradation processes such as hydrolysis of filler and lead to particle loss⁶⁹, which can be additionally accelerated due to the increased contact of water with particles at the matrix-filler interface when their compatibility is low. Water can migrate into the filler-matrix interface and into free spaces when particles were lost, increasing the WSO. An increase in the WSL values may also be related to the QA-PEI-NPs because of possible weaker interactions between filler particles and water molecules in comparison to those between QA-PEI-NPs and matrix. The leaching of particles may also increase the contact area of the matrix with the water, which intensified the leaching process of different components.

The water contact angle is discussed due to its influence on plaque formation because materials with high CA demonstrate less bacterial adherence⁹⁰. The results showed that the CA of the tested surfaces increased to 6% for the highest concentration of QA-PEI-NPs (other changes were insignificant), however, all values obtained were less than 90°, so the character of the surfaces was still hydrophilic⁹¹. The registered increase in CA can be caused by the presence of hydrophobic N-octyl substituents in QA-PEI-NPs⁴³.

Conclusions

The article provided new information on the properties of model composites based on the bis-GMA/UDMA/TEGDMA matrix reinforced with glass fillers and enriched with QA-PEI-NPs. The results showed that the compounding from 0.5 to 3% of QA-PEI-NPs allows to obtain high antimicrobial effectiveness and satisfactory biocompatibility. The QA-PEI-NPs introductions have no effect on the degree of conversion DC, Vickers microhardness, and flexural modulus' values and caused a favorable increase in contact angle. On the other hand, QA-PEI-NPs increased water sorption and solubility, decreased flexural strength, and compressive strength. The mentioned changes were insignificant and acceptable for most experimental composites, excluding the highest antibacterial filler content. Probably the reason for the deterioration of some properties was low compatibility between filler particles and the matrix; therefore, it is worth extending the research by surface modification of QA-PEI-NPs to achieve optimum performance characteristics.

Data availability

The datasets used and/or analyses during the current study available from the corresponding author on reasonable request.

Received: 21 November 2022; Accepted: 29 September 2023

Published online: 15 October 2023

References

- Vos, T. *et al.* Global, regional, and national incidence, prevalence, and years lived with disability for 310 diseases and injuries, 1990–2015: A systematic analysis for the Global Burden of Disease Study 2015. *Lancet* **388**, 1545–1602 (2016).
- Kassebaum, N. J. *et al.* Global, regional, and national prevalence, incidence, and disability-adjusted life years for oral conditions for 195 Countries, 1990–2015: A systematic analysis for the global burden of diseases, injuries, and risk factors. *J. Dent. Res.* **96**, 380–387 (2017).
- Merchan, M. T. & Ismail, A. I. Measurement and distribution of dental caries. In *Burt and Eklund's Dentistry, Dental Practice, and the Community* 7th edn (eds Mascarenhas, A. K. *et al.*) 154–170 (W. B. Saunders, 2021).
- Dursun, E., Fron-Chabouis, H., Attal, J.-P. & Raskin, A. Bisphenol A release: Survey of the composition of dental composite resins. *Open Dent. J.* **10**, 446–453 (2016).
- Ilie, N. & Hickel, R. Resin composite restorative materials. *Aust. Dent. J.* **56**(Suppl 1), 59–66 (2011).
- Ástvaldsdóttir, Á. *et al.* Longevity of posterior resin composite restorations in adults: A systematic review. *J. Dent.* **43**, 934–954 (2015).
- Alzraikat, H., Burrow, M., Maghaireh, G. & Taha, N. Nanofilled resin composite properties and clinical performance: A review. *Oper. Dent.* <https://doi.org/10.2341/17-208-T> (2018).
- Bernardo, M. *et al.* Survival and reasons for failure of amalgam versus composite posterior restorations placed in a randomized clinical trial. *J. Am. Dent. Assoc.* **138**, 775–783 (2007).
- Pallesen, U., van Dijken, J. W. V., Halken, J., Hallonsten, A.-L. & Høigaard, R. A prospective 8-year follow-up of posterior resin composite restorations in permanent teeth of children and adolescents in Public Dental Health Service: Reasons for replacement. *Clin. Oral Investig.* **18**, 819–827 (2014).
- Shih, W.-Y. Microleakage in different primary tooth restorations. *J. Chin. Med. Assoc.* **79**, 228–234 (2016).
- Sousa, R. P. *et al.* In situ effects of restorative materials on dental biofilm and enamel demineralisation. *J. Dent.* **37**, 44–51 (2009).
- Chatzistavrou, X. *et al.* Bactericidal and bioactive dental composites. *Front. Physiol.* **9**, 103 (2018).
- Zhang, N. *et al.* Do dental resin composites accumulate more oral biofilms and plaque than amalgam and glass ionomer materials?. *Materials* **9**, 888 (2016).
- Delaviz, Y., Finer, Y. & Santerre, J. P. Biodegradation of resin composites and adhesives by oral bacteria and saliva: A rationale for new material designs that consider the clinical environment and treatment challenges. *Dent. Mater.* **30**, 16–32 (2014).
- Lai, G. & Li, M. Secondary Caries. In *Contemporary Approach to Dental Caries* 403–422 (InTech, 2012).
- Maas, M. S. *et al.* Trends in restorative composites research: What is in the future?. *Braz. Oral Res.* **31**, e55 (2017).
- Sun, Q. *et al.* Recent progress in antimicrobial strategies for resin-based restoratives. *Polymers* **13**, 1590 (2021).
- Yin, I. X. *et al.* The antibacterial mechanism of silver nanoparticles and its application in dentistry. *Int. J. Nanomed.* **15**, 2555–2562 (2020).

19. Angel Villegas, N. *et al.* Novel antibacterial resin-based filling material containing nanoparticles for the potential one-step treatment of caries. *J. Healthc. Eng.* **2019**, 6367919 (2019).
20. Wang, Y. *et al.* Strong antibacterial dental resin composites containing cellulose nanocrystal/zinc oxide nanohybrids. *J. Dent.* **80**, 23–29 (2019).
21. Bai, X. *et al.* Preparation of Zn doped mesoporous silica nanoparticles (Zn-MSNs) for the improvement of mechanical and antibacterial properties of dental resin composites. *Dent. Mater.* **36**, 794–807 (2020).
22. Stencil, R. *et al.* Properties of experimental dental composites containing antibacterial silver-releasing filler. *Materials* **11**, 1031 (2018).
23. Dias, H. B., Bernardi, M. I. B., Bauab, T. M., Hernandez, A. C. & de Souza Rastelli, A. N. Titanium dioxide and modified titanium dioxide by silver nanoparticles as an anti biofilm filler content for composite resins. *Dent. Mater.* **35**, e36–e46 (2019).
24. Luo, D. *et al.* Gold nanorod mediated chlorhexidine microparticle formation and near-infrared light induced release. *Langmuir* **33**, 7982–7993 (2017).
25. Boaro, L. C. C. *et al.* Antibacterial resin-based composite containing chlorhexidine for dental applications. *Dent. Mater.* **35**, 909–918 (2019).
26. Lapinska, B. *et al.* An in vitro study on the antimicrobial properties of essential oil modified resin composite against oral pathogens. *Materials* **13**, E4383 (2020).
27. Hwang, G., Koltisko, B., Jin, X. & Koo, H. Nonleachable imidazolium-incorporated composite for disruption of bacterial clustering, exopolysaccharide-matrix assembly, and enhanced biofilm removal. *ACS Appl. Mater. Interfaces* **9**, 38270–38280 (2017).
28. Tanaka, C. B. *et al.* Development of novel dental restorative composites with dibasic calcium phosphate loaded chitosan fillers. *Dent. Mater.* **36**, 551–559 (2020).
29. Wang, Y., Zhu, M. & Zhu, X. X. Functional fillers for dental resin composites. *Acta Biomater.* **122**, 50–65 (2021).
30. Jiao, Y., Tay, F. R., Niu, L.-N. & Chen, J.-H. Advancing antimicrobial strategies for managing oral biofilm infections. *Int. J. Oral Sci.* **11**, 28 (2019).
31. Szram, A., Sokołowski, J., Nowak, J., Domarecka, M. & Łukomska-Szymańska, M. Mechanical properties of composite material modified with essential oil. *Inżynieria Materiałowa* **38**, 49–53 (2017).
32. Zhang, J. F. *et al.* Antibacterial dental composites with chlorhexidine and mesoporous silica. *J. Dent. Res.* **93**, 1283–1289 (2014).
33. Chrószcz, M. & Barszczewska-Rybarek, I. Nanoparticles of quaternary ammonium polyethylenimine derivatives for application in dental materials. *Polymers* **12**, 2551 (2020).
34. Beyth, N. *et al.* Surface antimicrobial activity and biocompatibility of incorporated polyethylenimine nanoparticles. *Biomaterials* **29**, 4157–4163 (2008).
35. Nuzhdina, A. V. *et al.* Simple and versatile method for creation of non-leaching antimicrobial surfaces based on cross-linked alkylated polyethylenimine derivatives. *Mater. Sci. Eng. C* **70**, 788–795 (2017).
36. Yew, P. Y. M. *et al.* Quarternized short polyethylenimine shows good activity against drug-resistant bacteria. *Macromol. Mater. Eng.* **302**, 1700186 (2017).
37. Yudovin-Farber, I., Beyth, N., Weiss, E. I. & Domb, A. J. Antibacterial effect of composite resins containing quaternary ammonium polyethylenimine nanoparticles. *J. Nanopart. Res.* **12**, 591–603 (2010).
38. Shvero, D. K., Zaltsman, N., Hazan, R., Weiss, E. I. & Beyth, N. Characterisation of the antibacterial effect of polyethylenimine nanoparticles in relation to particle distribution in resin composite. *J. Dent.* **43**, 287–294 (2015).
39. Beyth, N., Yudovin-Farber, I., Bahir, R., Domb, A. J. & Weiss, E. I. Antibacterial activity of dental composites containing quaternary ammonium polyethylenimine nanoparticles against *Streptococcus mutans*. *Biomaterials* **27**, 3995–4002 (2006).
40. Pietrokovski, Y., Nisimov, I., Kesler-Shvero, D., Zaltsman, N. & Beyth, N. Antibacterial effect of composite resin foundation material incorporating quaternary ammonium polyethylenimine nanoparticles. *J. Prosthet. Dent.* **116**, 603–609 (2016).
41. Beyth, N., Yudovin-Farber, I., Perez-Davidi, M., Domb, A. J. & Weiss, E. I. Polyethylenimine nanoparticles incorporated into resin composite cause cell death and trigger biofilm stress in vivo. *Proc. Natl. Acad. Sci. USA* **107**, 22038–22043 (2010).
42. Yudovin-Farber, I. *et al.* Surface characterization and biocompatibility of restorative resin containing nanoparticles. *Biomacromolecules* **9**, 3044–3050 (2008).
43. Barszczewska-Rybarek, I. M., Chrószcz, M. W. & Chladek, G. Physicochemical and mechanical properties of Bis-GMA/TEGDMA dental composite resins enriched with quaternary ammonium polyethylenimine nanoparticles. *Materials* **14**, 2037 (2021).
44. Yudovin-Farber, I., Golenser, J., Beyth, N., Weiss, E. I. & Domb, A. J. Quaternary ammonium polyethylenimine: Antibacterial activity. *J. Nanomater.* **2010**, e826343 (2010).
45. Festuccia, M. S. C. C., da Garcia, L. F. R., Cruvinel, D. R. & Pires-De-Souza, F. C. P. Color stability, surface roughness and micro-hardness of composites submitted to mouthrinsing action. *J. Appl. Oral. Sci.* **20**, 200–205 (2012).
46. ISO 10993-5 *Biological Evaluation of Medical Devices—Part 5: Tests for In Vitro Cytotoxicity*.
47. Barszczewska-Rybarek, I. & Jurczyk, S. Comparative study of structure-property relationships in polymer networks based on bis-GMA TEGDMA and various urethane-dimethacrylates. *Materials* **8**, 1230–1248 (2015).
48. Chladek, G. *et al.* Influence of aging solutions on wear resistance and hardness of selected resin-based dental composites. *Acta Bioeng. Biomech.* **18**, 43–52 (2016).
49. Galvão, M. R. *et al.* Compressive strength of dental composites photo-activated with different light tips. *Laser Phys.* **23**, 045604 (2013).
50. ISO International Organization for Standardization. *EN ISO 4049:2019 Dentistry—Polymer-Based Restorative Materials* (2019).
51. Domb, A. J., Weiss, E., Beyth, N., Farber, I. & Davidi, M. P. *Antimicrobial Nanoparticulate Additives Forming Non-leachable Sustained Antimicrobial Polymeric Compositions*. U.S. Patent 20080226728A1 18 September 2008. (2013).
52. Stencil, R. *et al.* Effects of different inorganic fillers on mechanical properties and degree of conversion of dental resin composites. *Arch. Metall. Mater.* **63**(3), 1361–1369 (2018).
53. Cazzaniga, G., Ottobelli, M., Ionescu, A., Garcia-Godoy, F. & Brambilla, E. Surface properties of resin-based composite materials and biofilm formation: A review of the current literature. *Am. J. Dent.* **28**, 311–320 (2015).
54. Sturz, C. R. C., Faber, F.-J., Scheer, M., Rothamel, D. & Neugebauer, J. Effects of various chair-side surface treatment methods on dental restorative materials with respect to contact angles and surface roughness. *Dent. Mater. J.* **34**, 796–813 (2015).
55. Chour, R. G. *et al.* Comparative evaluation of effect of different polishing systems on surface roughness of composite resin: An in vitro study. *J. Int. Soc. Prev. Community Dent.* **6**, S166–S170 (2016).
56. Abzal, M. S. *et al.* Evaluation of surface roughness of three different composite resins with three different polishing systems. *J. Conserv. Dent.* **19**, 171–174 (2016).
57. Hassan, A. M., Nabih, S. M., Mossa, H. M. & Baroudi, K. The effect of three polishing systems on surface roughness of flowable, microhybrid, and packable resin composites. *J. Int. Soc. Prev. Community Dent.* **5**, 242–247 (2015).
58. Tosco, V. *et al.* Effect of four different finishing and polishing systems on resin composites: roughness surface and gloss retention evaluations. *Minerva Stomatol.* **69**, 207–214 (2020).
59. Rigo, L. C. *et al.* Influence of polishing system on the surface roughness of flowable and regular-viscosity bulk fill composites. *Int. J. Periodont. Restor. Dent.* **38**, e79–e86 (2018).
60. Gilbert, P. & Moore, L. E. Cationic antiseptics: Diversity of action under a common epithet. *J. Appl. Microbiol.* **99**, 703–715 (2005).
61. Wang, L., Hu, C. & Shao, L. The antimicrobial activity of nanoparticles: Present situation and prospects for the future. *Int. J. Nanomed.* **12**, 1227–1249 (2017).

62. Sharmin, S. *et al.* Nanoparticles as antimicrobial and antiviral agents: A literature-based perspective study. *Heliyon* **7**, e06456 (2021).
63. Ortega, A. *et al.* Antimicrobial evaluation of quaternary ammonium polyethyleneimine nanoparticles against clinical isolates of pathogenic bacteria. *IET Nanobiotechnol.* **9**, 342–348 (2015).
64. Taylor, E. & Webster, T. J. Reducing infections through nanotechnology and nanoparticles. *Int. J. Nanomed.* **6**, 1463–1473 (2011).
65. Randolph, L. D. *et al.* Ultra-fast light-curing resin composite with increased conversion and reduced monomer elution. *Dent. Mater.* **30**, 594–604 (2014).
66. Barszczewska-Rybarek, I. M. A guide through the dental dimethacrylate polymer network structural characterization and interpretation of physico-mechanical properties. *Materials* **12**, 4057 (2019).
67. Atria, P. J. *et al.* Micro-computed tomography evaluation of volumetric polymerization shrinkage and degree of conversion of composites cured by various light power outputs. *Dent. Mater. J.* **37**, 33–39 (2018).
68. Oglakci, B. *et al.* The effect of curing modes and times of Third-Generation led LCU on the mechanical properties of nanocomposites. *Odovtos Int. J. Dent. Sci.* **24**, 61–74 (2022).
69. da Silva, E. M., Almeida, G. S., Poskus, L. T. & Guimarães, J. G. A. Relationship between the degree of conversion, solubility and salivary sorption of a hybrid and a nanofilled resin composite. *J. Appl. Oral Sci.* **16**, 161–166 (2008).
70. AlShaafi, M. M. Factors affecting polymerization of resin-based composites: A literature review. *Saudi Dent. J.* **29**, 48–58 (2017).
71. Brandão, N. L. *et al.* Model resin composites incorporating ZnO-NP: Activity against *S. mutans* and physicochemical properties characterization. *J. Appl. Oral Sci.* **26**, e20170270 (2018).
72. El-Tamimi, K. M., Bayoumi, D. A., Ahmed, M. M. Z., Albaijan, I. & El-Sayed, M. E. The effect of salinized nano ZrO₂ particles on the microstructure, hardness, and wear behavior of acrylic denture tooth nanocomposite. *Polymers* **14**, 302 (2022).
73. Vidal, M. L. *et al.* Physical and chemical properties of model composites containing quaternary ammonium methacrylates. *Dent. Mater.* **34**, 143–151 (2018).
74. Fuchi, K. *et al.* Electrodeposition behavior of Zn-polyethyleneimine composite from sulfate solution and its micro structure. *Mater. Trans.* **59**, 1767–1776 (2018).
75. Chladek, G. *et al.* Effect of storage in distilled water for three months on the antimicrobial properties of poly(methyl methacrylate) denture base material doped with inorganic filler. *Materials* **9**, 328 (2016).
76. Faria, A. C. L., Benassi, U. M., Rodrigues, R. C. S., Ribeiro, R. F. & da Mattos, M. Analysis of the relationship between the surface hardness and Wear resistance of indirect composites used as veneer materials. *Braz. Dent. J.* **18**, 60–64 (2007).
77. Korkut, E., Torlak, E. & Altunsoy, M. Antimicrobial and mechanical properties of dental resin composite containing bioactive glass. *J. Appl. Biomater. Funct. Mater.* **14**, e296-301 (2016).
78. Chang, M., Dennison, J. & Yaman, P. Physical property evaluation of four composite materials. *Oper. Dent.* **38**, E144-153 (2013).
79. Chun, K., Choi, H. & Lee, J. Comparison of mechanical property and role between enamel and dentin in the human teeth. *J. Dent. Biomech.* **5**, 208009 (2014).
80. Stanford, J. W., Weigel, K. V., Paffenbarger, G. C. & Sweeney, W. T. Compressive properties of hard tooth tissues and some restorative materials. *J. Am. Dent. Assoc.* **60**, 746–756 (1960).
81. Das Neves, P. B. A., Agnelli, J. A. M., Kurachi, C. & de Souza, C. W. O. Addition of silver nanoparticles to composite resin: effect on physical and bactericidal properties in vitro. *Braz. Dent. J.* **25**, 141–145 (2014).
82. Niu, L. N. *et al.* Tetrapod-like zinc oxide whisker enhancement of resin composite. *J. Dent. Res.* **89**, 746–750 (2010).
83. Tavassoli Hojati, S. *et al.* Antibacterial, physical and mechanical properties of flowable resin composites containing zinc oxide nanoparticles. *Dent. Mater.* **29**, 495–505 (2013).
84. Pratap, B., Gupta, R. K., Bhardwaj, B. & Nag, M. Resin based restorative dental materials: Characteristics and future perspectives. *Jpn. Dent. Sci. Rev.* **55**, 126–138 (2019).
85. Rodrigues Junior, S. A., Zanchi, C. H., de Carvalho, R. V. & Demarco, F. F. Flexural strength and modulus of elasticity of different types of resin-based composites. *Braz. Oral Res.* **21**, 16–21 (2007).
86. Ferracane, J. L. Resin-based composite performance: Are there some things we can't predict?. *Dent. Mater.* **29**, 51–58 (2013).
87. Kumar, N. & Sangi, L. Water sorption, solubility, and resultant change in strength among three resin-based dental composites. *J. Investig. Clin. Dent.* **5**, 144–150 (2014).
88. Mortier, E., Gerdolle, D. A., Jacquot, B. & Panighi, M. M. Importance of water sorption and solubility studies for couple bonding agent–resin-based filling material. *Oper. Dent.* **29**, 669–676 (2004).
89. Bociong, K. *et al.* The influence of water sorption of dental light-cured composites on shrinkage stress. *Materials* **10**, 1142 (2017).
90. Rüttermann, S., Beikler, T. & Janda, R. Contact angle and surface free energy of experimental resin-based dental restorative materials after chewing simulation. *Dent. Mater.* **30**, 702–707 (2014).
91. Liber-Kneć, A. & Lagan, S. Surface testing of dental biomaterials-determination of contact angle and surface free energy. *Materials* **14**, 2716 (2021).

Acknowledgements

We would like to thank ARKONA Laboratory Of Dental Pharmacology, Poland for technical support during the research.

Author contributions

Conceptualization, G.C. and I.B.-R.; methodology, all authors; investigation, G.C., M.C.-P., and A.M.; resources, all authors; data curation, G.C., M.C.-P. and A.M.; writing—original draft G.C., M.C.-P. and A.M.; writing—review and editing, G.C. and I.B.-R.; supervision, G.C. and I.B.-R.; project administration and funding acquisition, G.C. and I.B.-R.

Funding

Publication supported as part of the Excellence Initiative—Research University program implemented at the Silesian University of Technology, year 2021/2023 (Grant Number: 10/010/SDU/10-21-03) and by the Rector's pro-quality grant (Silesian University of Technology, Grant Number: 10/010/RGJ23/1140).

Competing interests

The authors declare no competing interests.

Additional information

Supplementary Information The online version contains supplementary material available at <https://doi.org/10.1038/s41598-023-43851-y>.

Correspondence and requests for materials should be addressed to G.C.

Reprints and permissions information is available at www.nature.com/reprints.

Publisher's note Springer Nature remains neutral with regard to jurisdictional claims in published maps and institutional affiliations.



Open Access This article is licensed under a Creative Commons Attribution 4.0 International License, which permits use, sharing, adaptation, distribution and reproduction in any medium or format, as long as you give appropriate credit to the original author(s) and the source, provide a link to the Creative Commons licence, and indicate if changes were made. The images or other third party material in this article are included in the article's Creative Commons licence, unless indicated otherwise in a credit line to the material. If material is not included in the article's Creative Commons licence and your intended use is not permitted by statutory regulation or exceeds the permitted use, you will need to obtain permission directly from the copyright holder. To view a copy of this licence, visit <http://creativecommons.org/licenses/by/4.0/>.

© The Author(s) 2023